

Application of the rescaling model at small Bjorken x values

A.V. Kotikov^{1,3}, B.G. Shaikhatdenov³, Pengming Zhang^{1,2}

¹ Institute of Modern Physics, Lanzhou 730000, China

² University of Chinese Academy of Sciences, Yuquanlu 19A, Beijing 100049, China

³ Joint Institute for Nuclear Research, 141980, Dubna, Russia

October 20, 2018

Abstract

The Bessel-inspired behavior of parton densities at small Bjorken x values, obtained in the case of the flat initial conditions for DGLAP evolution equations, is used along with “frozen” and analytic modifications of the strong coupling constant to study the so-called EMC effect. Among other results, this approach allowed predicting small x behavior of the gluon density in nuclei.

Keywords: Deep inelastic scattering; parton densities; EMC effect.

1 Introduction

The study of deep-inelastic scattering (DIS) of leptons off nuclei reveals an appearance of a significant nuclear effect (for a review see, e.g., [1, 2]). It was first observed by the European Muon Collaboration [3] in the valence quark dominance region; hence the name. This observation rules out the naive picture of a nucleus as being a system of quasi-free nucleons.

There in general are two mainstream approaches to studying the EMC effect. In the first one, which is at present more popular, nuclear parton distribution functions (nPDFs) are extracted from the global fits to nuclear data by using empirical parametrizations of their normalizations (see [4, 5, 6]). This is completely analogous to respective studies of usual (nucleon) PDFs (see recent analyses in [7]). Both PDFs and nPDFs are obtained from the numerical solution to Dokshitzer-Gribov-Lipatov-Altarelli-Parisi (DGLAP) equations [8]¹. The second strategy is based upon some models of nuclear PDFs (see different models in, for example, [11]–[14] and a recent review [16]).

Here we will follow the rescaling model [13, 14], which was very popular some time ago. The model is based on a suggestion [15] that the effective confinement size of gluons and quarks in the nucleus is greater than in a free nucleon. In the framework of perturbative QCD it was found [13, 14, 15] that such a change in the confinement scale predicts that nPDFs and PDFs can be related by simply rescaling their arguments (see Eq. (8) below). Thus, in a sense, the rescaling model lies in-between two above approaches: in its framework there are certain relations between usual and nuclear PDFs that result from shifting the values of kinematical variable μ^2 ; however, both densities obey DGLAP equations.

At that time, the model was established for the valence quark dominance region $0.2 \leq x \leq 0.8$. The aim of our paper is to extend its applicability to the region of small x values,

¹Sometimes, in the analyses of DIS experimental data it is convenient to use an exact solution to DGLAP equations in the Mellin moment space and reconstruct SF F_2 from the moments (see recent paper [9] and references and discussions therein). The studies of nuclear effects in such a type of analyses can be found in [10], though its consideration is beyond the scope of the present study.

where the rescaling values can be different for gluons and quarks. To see it clearly we use the generalized double-scaling approach (DAS) [17, 18]. The latter is based upon the analytical solution to DGLAP equations in the small x region and generalizes earlier studies [19].

A few years ago most analyses of nPDFs have been done in the leading order (LO) of perturbation theory, but now the situation is drastically changed and the standard level of accuracy in current analyses is at the next-to-leading order (NLO) one (see [4, 5]). Even more, there have already appeared a global analysis [6] performed at the next-to-next-to-leading order. Nevertheless the present analysis will be carried out in LO. We note that the analysis to this level of accuracy is just for the start and can be considered as a first step in our investigations in this direction. We are going to improve the accuracy at least to the NLO level in the future works.

2 SF F_2 at low x

A reasonable agreement between HERA data [20] and predictions made by perturbative Quantum Chromodynamics (QCD) was observed for $Q^2 \geq 2 \text{ GeV}^2$ [21], thereby promising that perturbative QCD is capable of describing the evolution of parton densities down to very low Q^2 values.

Some time ago ZEUS and H1 Collaborations have presented new precise combined data [22] on the structure function (SF) F_2 . An application of the generalized DAS approach [18] at NLO shows that theoretical predictions are well compatible with experimental data at $Q^2 \geq 3 \div 4 \text{ GeV}^2$ (see recent results in [23]).

In the present paper we perform a LO analysis of the combined data [22] where the SF F_2 has the following form

$$F_2(x, \mu^2) = e f_q(x, \mu^2), \quad (1)$$

where $e = (\sum_1^f e_i^2)/f$ is an average of the squared quark charges. Notice that the approach used in these analyses will be analogous to that exploited in NLO ones carried out in [23]–[25].

The small- x asymptotic expressions for parton densities f_a can be written as follows

$$\begin{aligned} f_a(x, \mu^2) &= f_a^+(x, \mu^2) + f_a^-(x, \mu^2), \quad (\text{hereafter } a = q, g) \\ f_g^+(x, \mu^2) &= \left(A_g + \frac{4}{9} A_q \right) \tilde{I}_0(\sigma) e^{-\bar{d}_+ s} + O(\rho), \\ f_q^+(x, \mu^2) &= \frac{f}{9} \left(A_g + \frac{4}{9} A_q \right) \rho \tilde{I}_1(\sigma) e^{-\bar{d}_+ s} + O(\rho), \end{aligned} \quad (2)$$

$$f_g^-(x, \mu^2) = -\frac{4}{9} A_q e^{-d_- s} + O(x), \quad f_q^-(x, \mu^2) = A_q e^{-d_-(1)s} + O(x), \quad (3)$$

where I_ν ($\nu = 0, 1$) are the modified Bessel functions with

$$\begin{aligned} s &= \ln \left(\frac{a_s(\mu_0^2)}{a_s(\mu^2)} \right), \quad \sigma = 2 \sqrt{\left| \hat{d}_+ \right| s \ln \left(\frac{1}{x} \right)}, \quad \rho = \frac{\sigma}{2 \ln(1/x)}, \\ a_s(\mu^2) &\equiv \frac{\alpha_s(\mu^2)}{4\pi} = \frac{1}{\beta_0 \ln(\mu^2/\Lambda_{\text{LO}}^2)} \end{aligned} \quad (4)$$

and

$$\hat{d}_+ = -\frac{12}{\beta_0}, \quad \bar{d}_+ = 1 + \frac{20f}{27\beta_0}, \quad d_- = \frac{16f}{27\beta_0} \quad (5)$$

denote singular \hat{d}_+ and regular \bar{d}_+ parts of the “anomalous dimensions” $d_+(n)$ and $d_-(n)$ ², respectively, in the limit $n \rightarrow 1$.

²Note that the variables $d_\pm(n)$ are ratios $\gamma_\pm^{(\text{LO})}(n)/(2\beta_0)$ of LO anomalous dimensions $\gamma_\pm^{(\text{LO})}(n)$ and LO coefficient β_0 of QCD β -function.

By using the expressions given above we have analyzed H1 and ZEUS data for F_2 [22]. In order to keep the analysis as simple as possible, here we take $\mu^2 = Q^2$ and $\alpha_s(M_Z^2) = 0.1168$ in agreement with ZEUS results presented in [20]. Moreover, we use the fixed flavor scheme with two different values $f = 3$ and $f = 4$ of active quarks.

As can be seen from Table 1, the twist-two approximation looks reasonable for $Q^2 \geq 3.5$ GeV². It is almost completely compatible with NLO analyses done in [23]–[25]. Moreover, these results are rather close to original analyses (see [26] and references therein) performed by the HERAPDF group. As in the case of [26] our $\chi^2/DOF \sim 1$ unless combined H1 and ZEUS experimental data analyzed are kept according to $Q^2 \geq 3.5$ GeV².

At lower Q^2 there is certain disagreement, which is we believe to be explained by the higher-twist (HT) corrections playing their important role. These HT corrections have rather cumbersome form at low x [24]. As it was shown [25], it is very promising to use infrared modifications of the strong coupling constant in our analysis. Such types of coupling constants modify the low μ^2 behavior of parton densities and structure functions. What is important, they do not generate additional free parameters. Moreover, the present results will be applied in the analyses of NMC data (see Sect. 5 and 6) accumulated at very low Q^2 values, where the HT expansion ($\sim 1/Q^{2n}$) is thought to be not applicable.

So, following [25], we are going to use the so-called “frozen” $a_{\text{fr}}(\mu^2)$ [27] and analytic $a_{\text{an}}(\mu^2)$ [28] versions

$$a_{\text{fr}}(\mu^2) = a_s(\mu^2 + M_g^2), \quad a_{\text{an}}(\mu^2) = a_s(\mu^2) - \frac{1}{\beta_0} \frac{\Lambda_{\text{LO}}^2}{\mu^2 - \Lambda_{\text{LO}}^2}, \quad (6)$$

where M_g is a gluon mass with $M_g=1$ GeV² (see [29] and references therein ³).

It is seen that the results of the fits carried out when $a_{\text{fr}}(\mu^2)$ and $a_{\text{an}}(\mu^2)$ are used, are very similar to the corresponding ones obtained in [23]. Moreover, note that the fits in the cases with “frozen” and analytic strong coupling constants look very much alike (see also [25, 31]) and describe fairly well the data in the low Q^2 region, as opposed to the fits with a standard coupling constant, which largely fails here. The results are presented in Table 1. With the number of active quarks $f = 4$, they are shown also in Fig. 1.

Just like the previous analyses [23, 25, 31] we observe strong improvement in the agreement between theoretical predictions and experimental data once “frozen” and analytic modifications to the coupling constant are applied. When the data are cut by $Q^2 \geq 1$ GeV², χ^2 value drops by more than two times. Ditto for the analyses of data with $Q^2 \geq 3.5$ GeV² imposed.

Table 1.

$f = 3$ $Q^2 \geq$	$a_s(Q^2)$ 1 GeV ²	$a_s(Q^2)$ 3.5 GeV ²	$a_{\text{an}}(Q^2)$ 1 GeV ²	$a_{\text{an}}(Q^2)$ 3.5 GeV ²	$a_{\text{fr}}(Q^2)$ 1 GeV ²	$a_{\text{fr}}(Q^2)$ 3.5 GeV ²
A_g	0.46 ± 0.02	0.74 ± 0.04	1.16 ± 0.03	1.30 ± 0.04	0.96 ± 0.03	1.06 ± 0.04
A_q	1.58 ± 0.04	1.48 ± 0.06	1.16 ± 0.04	1.21 ± 0.07	1.23 ± 0.08	1.32 ± 0.07
Q_0^2	0.40 ± 0.01	0.46 ± 0.01	0.20 ± 0.01	0.16 ± 0.01	0.49 ± 0.01	0.53 ± 0.01
χ^2	365.7	69.7	149.7	42.9	140.4	47.6
$f = 4$ $Q^2 \geq$	$a_s(Q^2)$ 1 GeV ²	$a_s(Q^2)$ 3.5 GeV ²	$a_{\text{an}}(Q^2)$ 1 GeV ²	$a_{\text{an}}(Q^2)$ 3.5 GeV ²	$a_{\text{fr}}(Q^2)$ 1 GeV ²	$a_{\text{fr}}(Q^2)$ 3.5 GeV ²
A_g	0.47 ± 0.02	0.54 ± 0.03	0.65 ± 0.02	0.76 ± 0.03	0.96 ± 0.03	0.77 ± 0.03
A_q	1.58 ± 0.04	1.09 ± 0.06	0.95 ± 0.03	0.96 ± 0.04	1.23 ± 0.05	0.95 ± 0.06
Q_0^2	0.40 ± 0.01	0.37 ± 0.01	0.16 ± 0.01	0.19 ± 0.01	0.49 ± 0.01	0.43 ± 0.01
χ^2	366.0	57.0	166.3	43.6	140.0	40.6

Recent NLO analyses (see the third paper in [23]) have been carried out within the framework of the fixed flavor scheme with $f = 3$ active light flavors and with a purely perturbative

³There are a number of various approaches to define the value of this gluon mass and even the form of its momentum dependence (see, e.g., a recent review [30]).

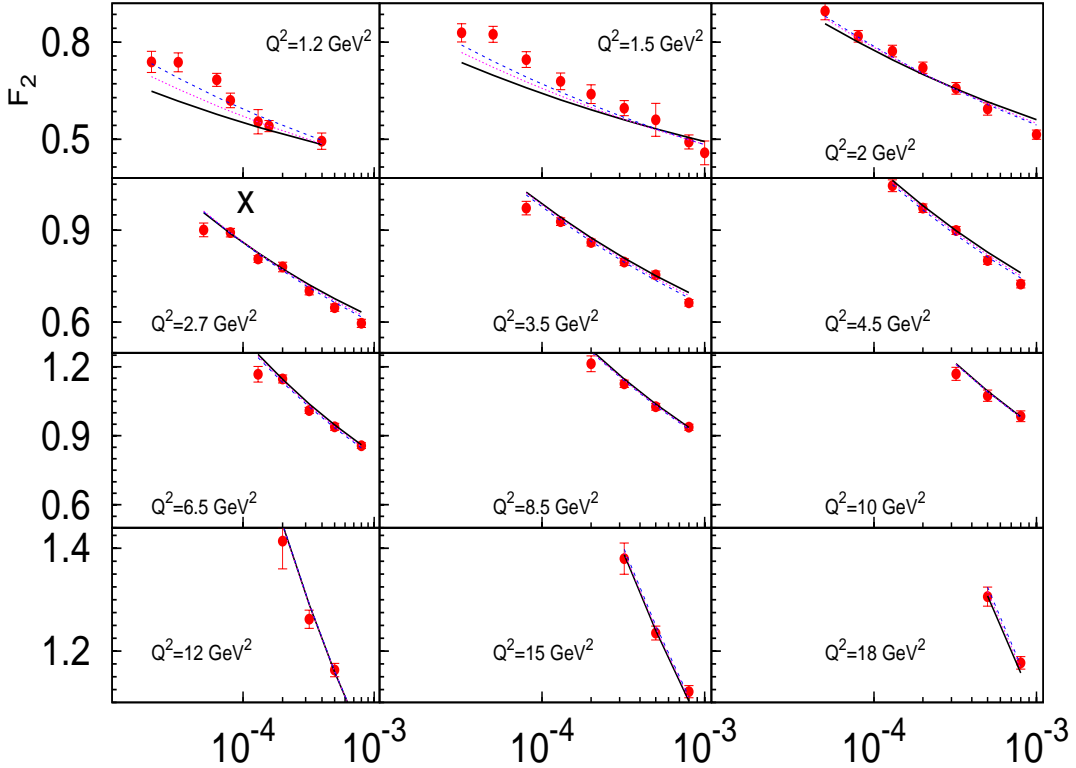


Figure 1: x dependence of $F_2(x, Q^2)$ in bins of Q^2 . The combined experimental data from H1 and ZEUS Collaborations [22] are compared with the LO fits for $Q^2 \geq 1$ GeV² implemented with a standard strong coupling constant (solid lines), and its frozen (dash-dotted lines) and analytic (dashed lines) modifications.

charm quark generated in a photon-gluon fusion (PGF) process. Such type of analyses for the complete SF $F_2(x, Q^2)$ cannot be done at LO.⁴

Therefore, we should use some fixed values of active quarks. Nevertheless, we would like to note that the results obtained here and those in [23]–[25], where various schemes were used, are very stable and close to each other.

3 Rescaling model

In the rescaling model [14] SF F_2 and, therefore, valence part of quark densities, gets modified in the case of a nucleus A at intermediate and large x values ($0.2 \leq x \leq 0.9$) as follows

$$F_2^A(x, \mu^2) = F_2(x, \mu_{A,v}^2), \quad f_{NS}^A(x, \mu^2) = f_{NS}(x, \mu_{A,v}^2), \quad (7)$$

where a new scale $\mu_{A,v}^2$ is related with μ^2 as

$$\mu_{A,v}^2 = \xi_v^A(\mu^2) \mu^2, \quad \xi_v^A(\mu^2) = \left(\frac{\lambda_A^2}{\lambda_N^2} \right)^{a_s(\tilde{\mu}^2)/a_s(\mu^2)} \quad (8)$$

where some additional scale $\tilde{\mu}^2 = 0.66$ GeV², which was in its turn an initial point in a μ^2 -evolution performed in [14]; it is then estimated in Appendix A of that paper. The quantity

⁴Notice that the SF $F_{2c}(x, Q^2)$, the charm part of $F_2(x, Q^2)$, appears with $a_s(Q^2)$ and can be confronted already at LO with the data produced in a PGF process (see Sect. 7 below).

λ_A/λ_N stands for the ratio of quark confinement radii in a nucleus A and nucleon. The values of λ_A/λ_N and $\xi_v^A(\mu^2)$ at $\mu^2 = 20 \text{ GeV}^2$ were evaluated for different nuclei and presented in Tables I and II in [14].

Since the factor $\xi_v^A(\mu^2)$ is μ^2 dependent, it is convenient to transform it to some μ^2 independent one. To this end, we consider the variable $\ln(\mu_{A,v}^2/\Lambda^2)$, which has the following form (from Eq. (8))

$$\ln\left(\frac{\mu_{A,v}^2}{\Lambda^2}\right) = \ln\left(\frac{\mu^2}{\Lambda^2}\right) \cdot (1 + \delta_v^A) \quad (9)$$

where the nuclear correction factor δ_v^A becomes μ^2 independent:

$$\delta_v^A = \frac{1}{\ln(\tilde{\mu}^2/\Lambda^2)} \ln\left(\frac{\lambda_A^2}{\lambda_N^2}\right), \quad (10)$$

where it is seen that two parameters, namely, the scale $\tilde{\mu}$ and ratio λ_A/λ_N , are combined to form a Q^2 -independent quantity. Using Eqs. (9) and/or (10), we can recover results for δ_v^A , which are presented in Table 2.

Table 2.

A N	${}^2\text{D}$	${}^4\text{He}$ 11	${}^7\text{Li}$ 16	${}^{12}\text{C}$ 16	${}^{40}\text{Ca}$ 11
δ_v^A	0.01	0.06	0.05	0.08	0.11
δ_v^{AD}	0	0.05	0.04	0.07	0.10
$-\delta_{+,an}^{AD}$	0	0.06 ± 0.01	0.06 ± 0.01	0.11 ± 0.01	0.19 ± 0.01
$-\delta_{-,an}^{AD}$	0	0.24 ± 0.08	0.22 ± 0.07	0.41 ± 0.04	0.51 ± 0.04
χ_{an}^2	0	4.68	17	9.68	12
$-\delta_{+,fr}^{AD}$	0	0.06 ± 0.01	0.06 ± 0.01	0.12 ± 0.01	0.21 ± 0.02
$-\delta_{-,fr}^{AD}$	0	0.32 ± 0.08	0.28 ± 0.07	0.54 ± 0.04	0.71 ± 0.04
χ_{fr}^2	0	5	35	26	37

Since our parton densities contain the variable s defined in Eq. (4), it is convenient to consider its A modification. It has the following simple form:

$$s_v^A \equiv \ln\left(\frac{\ln(\mu_{A,v}^2/\Lambda^2)}{\ln(\mu_0^2/\Lambda^2)}\right) = s + \ln(1 + \delta_v^A) \approx s + \delta_v^A, \quad (11)$$

i.e. the nuclear modification of the basic variable s depends on the μ^2 independent parameter δ_v^A , which possesses very small values.

4 Rescaling model at low x

Standard evidence coming from earlier studies contains conclusion about inapplicability of the rescaling model at small x values (see, for example, [32]). It looks like it can be related with some simplifications of low x analyses (see, for example, [33], where the rise in EMC ratio was wrongly predicted at small x values).

Using an accurate study of DGLAP equations at low x within the framework of the generalized DAS approach, it is possible to achieve nice agreement with the experimental data for the DIS structure function F_2 (see previous section)⁵. Therefore, we believe that all these indicate toward success in describing the EMC ratio by using the same approach.

We note that the main difference between global fits and DAS approach is in the restriction of applicability of the latter by low x region only, while the advantage of the DAS approach lies in the analytic solution to DGLAP equations.

⁵Moreover, using an analogous approach, good agreement was also found with the corresponding data for jet multiplicities [34].

Thus, we are trying to apply the DAS approach to low x region of EMC effect using a simple fact that the rise of parton densities increases with increasing Q^2 values. This way, with scales of PDF evolutions less than Q^2 (i.e. $\mu^2 \leq Q^2$) in nuclear cases, we can directly reproduce the shadowing effect which is observed in the global fits. Since there are two components (2) for each parton density, we have two free parameters μ_{\pm} to be fit in the analyses of experimental data for EMC effect at low x values.

An application of the rescaling model at low x can be incorporated at LO as follows:

$$\begin{aligned} F_2^A(x, \mu^2) &= e f_q^A(x, \mu^2), \quad F_2^N(x, \mu^2) = e f_q(x, \mu^2), \\ f_a^A(x, \mu^2) &= f_a^{A,+}(x, \mu^2) + f_a^{A,-}(x, \mu^2), \quad (a = q, g), \quad f_a^{A,\pm}(x, \mu^2) = f_a^{\pm}(x, \mu_{A,\pm}^2), \end{aligned} \quad (12)$$

with a similar definition of $\mu_{A,\pm}^2$ as in the previous section (up to replacement $v \rightarrow \pm$). The expressions for $f_a^{\pm}(x, \mu^2)$ are given in Eqs. (2) and (3).

Then, the corresponding values of s_{\pm}^A are found to be

$$s_{\pm}^A \equiv \ln \left(\frac{\ln(\mu_{A,\pm}^2/\Lambda^2)}{\ln(\mu_0^2/\Lambda^2)} \right) = s + \ln(1 + \delta_{\pm}^A), \quad (13)$$

because of the saturation at low x values for all considered Q^2 values, which in our case should be related with decreasing the arguments of “ \pm ” component. Therefore, the values of δ_{\pm}^A should be negative.

5 Analysis of the low x data for nucleus

Note that it is usually convenient to study the following ratio (see Fig. 1 in Ref. [16])

$$R_{F_2}^{AD}(x, \mu^2) = \frac{F_2^A(x, \mu^2)}{F_2^D(x, \mu^2)}. \quad (14)$$

Using the fact that the nuclear effect in a deuteron is very small (see Table 1 for the values of δ_v^A and discussions in [16])⁶, we can suggest that

$$\begin{aligned} F_2^D(x, \mu^2) &= e f_q(x, \mu^2), \quad F_2^A(x, \mu^2) = e \bar{f}_q^A(x, \mu^2), \\ \bar{f}_a^A(x, \mu^2) &= \bar{f}_a^{A,+}(x, \mu^2) + \bar{f}_a^{A,-}(x, \mu^2), \quad (a = q, g), \quad \bar{f}_a^{A,\pm}(x, \mu^2) = f_a^{\pm}(x, \mu_{AD,\pm}^2), \end{aligned} \quad (15)$$

i.e.

$$\begin{aligned} \bar{f}_g^{A,+}(x, \mu^2) &= \left(A_g + \frac{4}{9} A_q \right) I_0(\sigma_+^{AD}) e^{-\bar{d}_+ s_+^{AD}} + O(\rho_+^{AD}), \\ \bar{f}_q^{A,+}(x, \mu^2) &= \frac{f}{9} \left(A_g + \frac{4}{9} A_q \right) \rho_+^{AD} I_1(\sigma_+^{AD}) e^{-\bar{d}_+ s_+^{AD}} + O(\rho_+^{AD}), \end{aligned} \quad (16)$$

$$\bar{f}_g^{A,-}(x, \mu^2) = -\frac{4}{9} A_q e^{-d_- s_-^{AD}} + O(x), \quad \bar{f}_q^{A,-}(x, \mu^2) = A_q e^{-d_- (1) s_-^{AD}} + O(x), \quad (17)$$

where

$$\begin{aligned} \sigma_+^{AD} &= \sigma(s \rightarrow s_+^{AD}), \quad \rho_+^{AD} = \rho(s \rightarrow s_+^{AD}), \\ s_{\pm}^{AD} &\equiv \ln \left(\frac{\ln(\mu_{AD,\pm}^2/\Lambda^2)}{\ln(\mu_0^2/\Lambda^2)} \right) = s + \ln(1 + \delta_{\pm}^{AD}). \end{aligned} \quad (18)$$

We obtain the values of δ_+^{AD} and δ_-^{AD} by fitting NMC experimental data [36] for the EMC ratio at low x in the case of different nuclei. Since the experimental data for lithium and carbon are most precise and contain the maximal number of points (16 points for each nucleus), we perform combined fits of these data. Obtained results (with $\chi_{an}^2=27$ and $\chi_{fr}^2=43$ for 32 points) are presented in Table 3 and shown in Fig. 2.

⁶The study of nuclear effects in a deuteron can be found in [35], which also contains short reviews of preliminary investigations.

Table 3.

	$-\delta_{+,an}^{AD}$	$-\delta_{-,an}^{AD}$	$-\delta_{+,fr}^{AD}$	$-\delta_{-,fr}^{AD}$
${}^7\text{Li}$	0.061 ± 0.006	0.216 ± 0.065	0.073 ± 0.012	0.348 ± 0.067
${}^{12}\text{C}$	0.105 ± 0.007	0.411 ± 0.042	0.139 ± 0.013	0.590 ± 0.041

As can be seen in Fig. 2 there is large difference between the fits with “frozen” and analytic versions of the strong coupling constant. This is in contrast with the analysis done in Section 1 and results done in the earlier papers [31]. It seems that this difference comes about because we include in the analysis the region of very low Q^2 values, where “frozen” and analytic strong coupling constants are observed to be rather different (see also [29]).

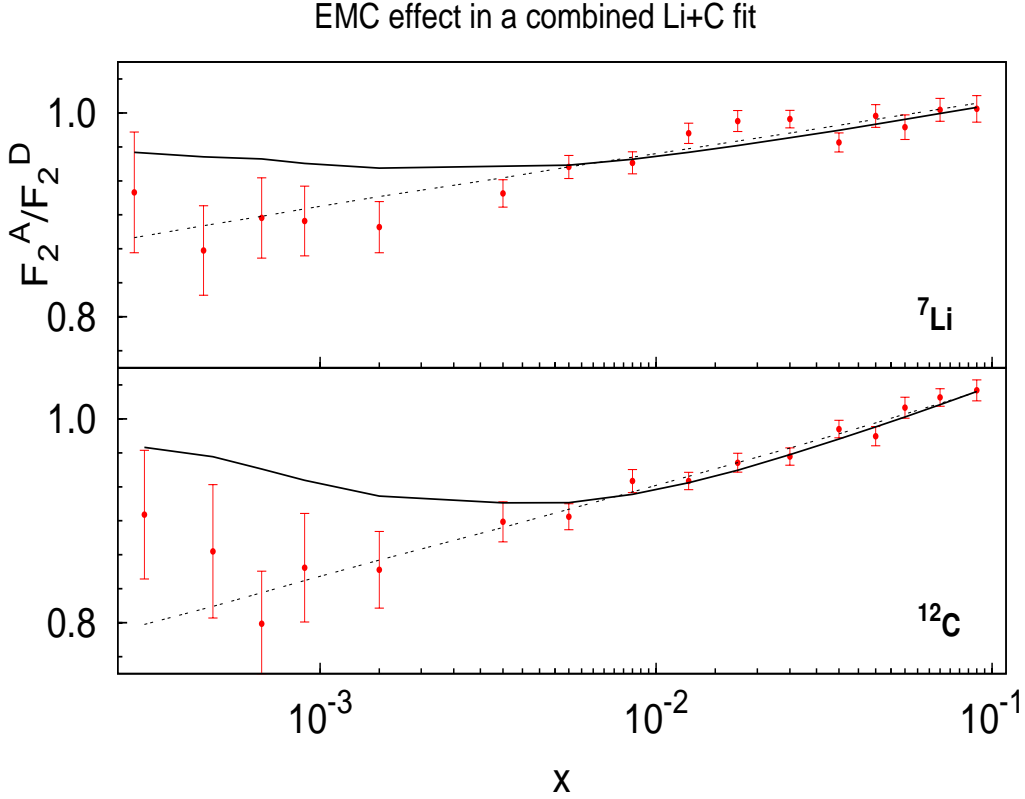


Figure 2: small x dependence of $R_a^{AD}(x, \mu^2)$ for lithium and carbon. The combined experimental data from NMC [36] are fitted by LO expressions implemented with the frozen (solid lines) and analytic (dashed lines) modifications of the strong coupling constant.

6 A dependence at low x

Taking NMC experimental data [36] along with E665 and HERMES Collaborations [37] for the EMC ratio at low x in the case of different nuclei, we can find the A dependence of δ_{\pm}^{AD} , which can be parameterized as follows

$$-\delta_{\pm}^{AD} = c_{\pm}^{(1)} + c_{\pm}^{(2)} A^{1/3}. \quad (19)$$

As it was already mentioned in the previous section, usage of the analytic coupling constant leads to the fits with smaller χ^2 values. For example, the values of $c_{\pm}^{(1)}$ and $c_{\pm}^{(2)}$ found in the

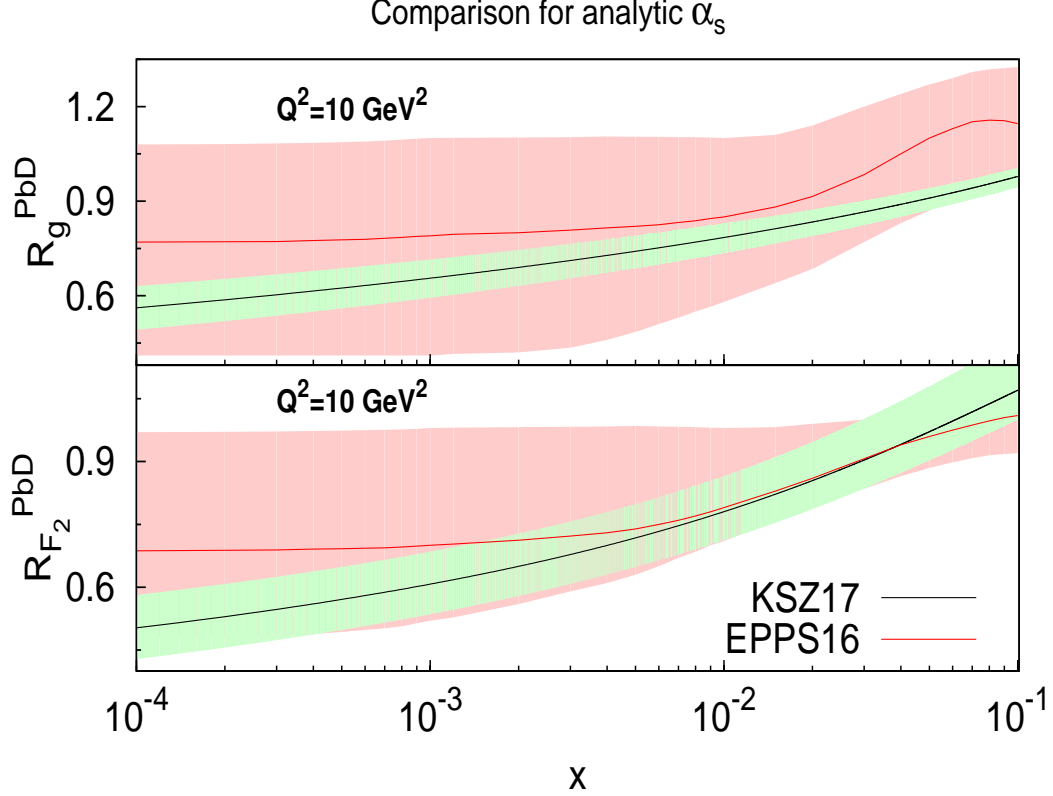


Figure 3: x dependence of $R_{F_2}^{AD}(x, \mu^2)$ and $R_g^{AD}(x, \mu^2)$ at $\mu^2=10 \text{ GeV}^2$ for lead data. A green line with pink band (shows 90% uncertainties) is taken from the second paper of [39], while a black one with light green band is obtained in the present paper.

combined fit of the data (76 points) when the analytic coupling constant is used (with $\chi^2 = 89$) look like

$$\begin{aligned} c_{+,an}^{(1)} &= -0.055 \pm 0.015, & c_{+,an}^{(2)} &= 0.068 \pm 0.006, \\ c_{-,an}^{(1)} &= 0.071 \pm 0.101, & c_{-,an}^{(2)} &= 0.120 \pm 0.039. \end{aligned} \quad (20)$$

Now, using the A dependence (19), $R_{F_2}^{AD}(x, \mu^2)$ values for any nucleus A can be predicted. What is more, we can consider also the ratios $R_a^{AD}(x, \mu^2)$ of parton densities in a nucleus and deuteron themselves,

$$R_a^{AD}(x, \mu^2) = \frac{\bar{f}_a^A(x, \mu^2)}{f_a(x, \mu^2)}, \quad (a = q, g), \quad (21)$$

with $\bar{f}_a^A(x, \mu^2)$ and $f_a(x, \mu^2)$ defined in Eqs. (15)–(19) and (2)–(5), respectively.

Indeed, at LO $R_q^{AD}(x, \mu^2) = R_{F_2}^{AD}(x, \mu^2)$; therefore, results for $R_q^{AD}(x, \mu^2)$ are already known. Since all the parameters of PDFs found within the framework of the generalized DAS approach are now fixed we can predict the ratio $R_g^{AD}(x, \mu^2)$ of the gluon densities in a nucleus and nucleon given in Eqs. (2), (3), (16) and (17), which is currently under intensive studies (see a recent paper [38] and review [39] along with references and discussion therein).

The results for $R_{F_2}^{AD}(x, \mu^2)$ and $R_g^{AD}(x, \mu^2)$, depicted in Fig. 3, show some difference between these ratios. It is also seen that the difference is similar to that obtained in a recent EPPS16 analysis (see the first paper in [5])⁷. However, what for $R_{F_2}^{AD}(x, \mu^2)$ and $R_g^{AD}(x, \mu^2)$

⁷ Note that the result for $R_g^{AD}(x, \mu^2)$ along with its uncertainty is completely determined by both the rescaling

themselves (irrespective of other results), we obtain a bit stronger effect at lowest x values, which does in fact not contradict the experimental data collected by the LHCb experiment (see recent review in [40]). Such a strong effect is also well compatible with the leading order EPPS09 analysis (which can also be found in [40]). It will be interesting to delve into more in-depth studies of the ratio $R_g^{AD}(x, \mu^2)$, which is one of our aims in the future.

7 SF F_{2c} at low x

Several years ago H1 [41] and ZEUS [42] Collaborations at HERA have separately presented their new data on the charm structure function F_{2c} ⁸ and more recently they have combined these data on $F_{2c}(x, \mu^2)$ [44]. The SF F_{2c} was found to be around 25% of F_2 , which is considerably larger than what was observed by the European Muon Collaboration (EMC) at CERN [45] at larger x values, where it was only around 1% of F_2 .

Ensuing and very extensive theoretical analyses were carried out to establish that the F_{2c} data can be described through the perturbative generation of charm in QCD [46]. In view of this, a PGF process in experiments with nucleon and nucleus targets is one of the most effective and promising studies of gluon density (see a recent review [47]).

Following [48] the SF F_{2c} at low x can be represented in the framework of the generalized DAS approach as follows

$$F_{2c}(x, \mu^2) = e_c^2 a_s(\mu_c) C_{2,g}(1, z_c(\mu^2)) f_g(x, \mu^2), \quad z_c(\mu^2) = \frac{m_c^2(\mu^2)}{\mu^2}, \quad e_c = \frac{2}{3}, \quad (22)$$

where $C_{2,g}(1, z_c(\mu^2))$ is a first Mellin moment of the LO PGF coefficient function $\tilde{C}_{2,g}(x, z_c(\mu^2))$. It can be obtained from the QED case [49] by adjusting the coupling constants (see also the direct calculations in [50, 51]). The Mellin moment $C_{2,g}(1, z_c(\mu^2))$ has a very compact form [48]:

$$C_{2,g}(1, z) = \frac{2}{3} \left[1 - \frac{2(1-z)}{\sqrt{1+4z}} \ln \frac{\sqrt{1+4z}-1}{\sqrt{1+4z}+1} \right]. \quad (23)$$

The gluon density $f_g(x, \mu^2)$ is determined in (2) and (3).

The scale μ_c in (22) is actually not fixed because the results for F_{2c} are at LO. There are two widespread scales, $\mu_c^2 = 4m_c^2$ [47, 52] and $\mu_c^2 = 4m_c^2 + \mu^2$ [41, 42, 44, 48]. We will use below both of them (see Subsect. 7.1).

In the framework of the rescaling model the SF $F_{2c}^A(x, \mu^2)$ for nucleus A can be represented as follows

$$F_{2c}^A(x, \mu^2) = e_c^2 \sum_{i=\pm} a_s(\mu_c(\mu_{A,i}^2)) C_{2,g}(1, z_c(\mu_{A,i}^2)) f_g^i(x, \mu_{A,i}^2), \quad (24)$$

where the scale $\mu_{A,i}^2$ looks like

$$\mu_{A,\pm}^2 = \Lambda^2 \left(\frac{\mu^2}{\Lambda^2} \right)^{1+\delta_{\pm}^A} = \mu^2 \left(\frac{\mu^2}{\Lambda^2} \right)^{\delta_{\pm}^A}, \quad (25)$$

as it follows from (7) with the replacement $v \rightarrow \pm$.

The results for the ratios $R_{F_2}^A(x, \mu^2)$, $R_g^A(x, \mu^2)$ and

$$R_c^A(x, \mu^2) = \frac{F_{2c}^A(x, \mu^2)}{F_{2c}(x, \mu^2)} \quad (26)$$

model and the analytic form for parton densities at low x values we've used. Therefore, it is clear that the light green band for $R_g^{AD}(x, \mu^2)$ should become broader due to a freedom in using various models. Also note that a comparison between two uncertainty bands shown in Fig. 3 is in some sense misleading. The pink band is much broader since the EPPS16 global analysis included a fit to all available data across quite a wide range in x as opposed to small x consideration adopted in the present paper. Nonetheless, we decided to quote it here just to give the reader an idea about the subject, at least qualitatively.

⁸Open charm production was also observed in the COMPASS fixed target experiment [43].

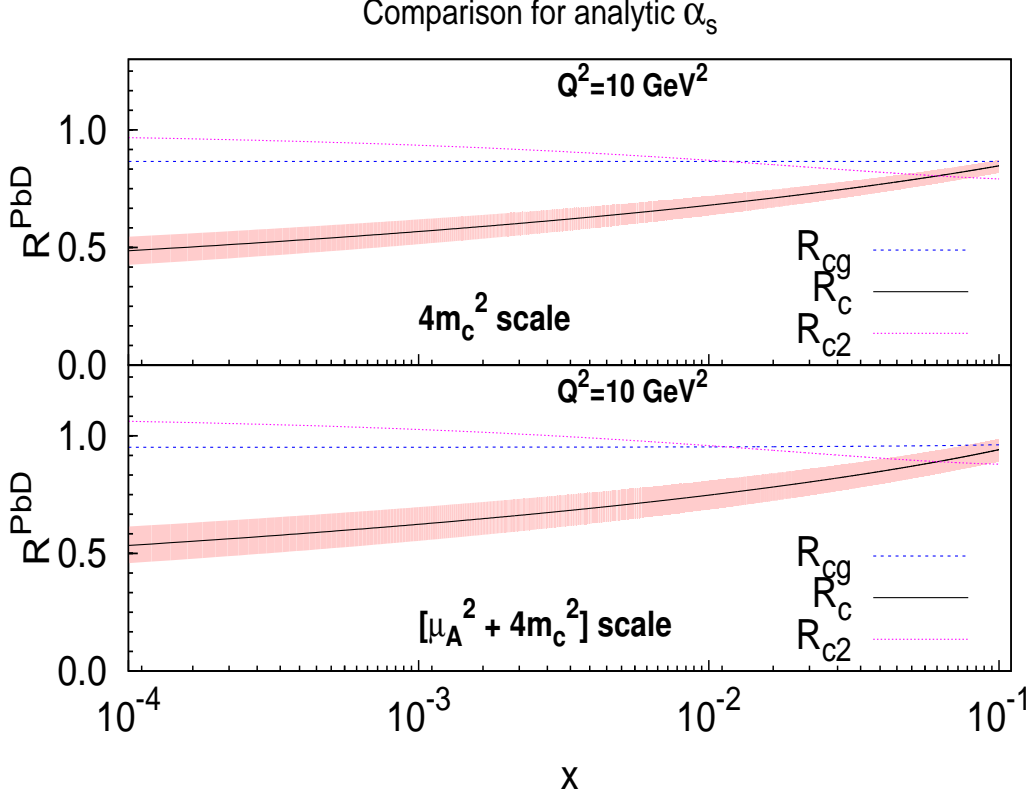


Figure 4: x dependence of $R_c^{AD}(x, \mu^2)$, $R_{cg}^{AD}(x, \mu^2)$ and $R_{c2}^{AD}(x, \mu^2)$ at $\mu^2=10$ GeV² for lead data and two choices of μ_c scale: $\mu_c^2 = 4m_c^2$ and $\mu_c^2 = 4m_c^2 + \mu^2$ are shown by black, blue and pink lines, respectively. A band represents 90% level uncertainties in determining $R_c^{AD}(x, \mu^2)$ values.

should be rather similar. Moreover, they have similar x -dependences, as it will be shown in the following subsection.

7.1 Analysis of the low x data

To have as close a relation with analyses in Sect. 5 as possible, let us consider the ratio

$$R_c^{AD}(x, \mu^2) = \frac{F_{2c}^A(x, \mu^2)}{F_{2c}^D(x, \mu^2)}. \quad (27)$$

As in Sect. 5, we will use the following expressions for the SFs

$$\begin{aligned} F_{2c}^D(x, \mu^2) &= e_c^2 a_s(\mu_c) C_{2,g}(1, a_c(\mu^2)) f_g(x, \mu^2), \\ F_{2c}^A(x, \mu^2) &= e_c^2 \sum_{i=\pm} a_s(\mu_c(\mu_{AD,i}^2)) C_{2,g}(1, z_c(\mu_{AD,i}^2)) \bar{f}_g^{A,\pm}(x, \mu^2), \end{aligned} \quad (28)$$

where the gluon density $\bar{f}_a^{A,\pm}(x, \mu^2) = f_a^\pm(x, \mu_{AD,\pm}^2)$ is defined in (16) and (17). The scale $\mu_{AD,\pm}^2$ can be obtained from (25) with the replacement $\delta_\pm^A \rightarrow \delta_\pm^{AD}$, by analogy with analyses in Sect. 5.

The results for the ratios $R_c^{AD}(x, \mu^2)$,

$$R_{cg}^{AD}(x, \mu^2) = \frac{R_c^{AD}(x, \mu^2)}{R_g^{AD}(x, \mu^2)} \quad \text{and} \quad R_{c2}^{AD}(x, \mu^2) = \frac{R_c^{AD}(x, \mu^2)}{R_{F2}^{AD}(x, \mu^2)} \quad (29)$$

are presented in Fig. 4 for $\mu^2 = 10$ GeV². Since the μ^2 -dependence of m_c is not strong, we use fixed $m_c = 1.27$ GeV [53] in our analysis.

As can be seen in Fig. 4, results look very much the same for both scales of μ_c . What is more, a behavior of the ratio $R_c^{AD}(x, \mu^2)$ is a little bit weaker than that of $R_{F_2}^{AD}(x, \mu^2)$ and a bit stronger than that observed for $R_g^{AD}(x, \mu^2)$. We hope that the x -dependence of the ratio $R_c^{AD}(x, \mu^2)$, along with that of $R_g^{AD}(x, \mu^2)$, can be measured at a future Electron–Ion Collider (see [47] and discussion therein).

8 Conclusion

Using a recent progress in the application of double-logarithmic approximations (see [18, 23] and [34]) to the studies of small x behavior of the structure and fragmentation functions, respectively, we applied the DAS approach [17, 18] to examine an EMC F_2 structure function ratio between various nuclei and a deuteron. Within a framework of the rescaling model [14, 15] good agreement between theoretical predictions and respective experimental data is achieved.

The theoretical formulæ contain certain parameters, whose values were fit in the analyses of experimental data. Once the fits are carried out we have predictions for the corresponding ratios of parton densities without free parameters. These results were used to predict small x behavior of the gluon density in nuclei, which is at present poorly known.

The ratios $R_a^{AD}(x, \mu^2)$ ($a = q, g$) predicted in the present paper are compatible with those given by various groups working in the area. From our point of view, it is quite valuable that the application of the rescaling model [14, 15] provided us with very simple forms for these ratios. It should also be mentioned that without any free parameters we can predict the ratio $R_c^{AD}(x, \mu^2)$ of charm parts, $F_{2c}^A(x, \mu^2)$ and $F_{2c}^D(x, \mu^2)$, of the respective structure functions. This latter ratio has a simple form and it is very similar to the corresponding ratio of the complete structure functions $F_2^A(x, \mu^2)$ and $F_2^D(x, \mu^2)$.

Following [18, 23] we plan to extend our analysis to the NLO level of approximation, the accuracy that is currently a standard in nPDF studies. Also, we are going to consider a rather broad range of the Bjorken variable x by using parametrizations of parton densities, which will be constructed by analogy with the one obtained earlier in the valence quark case (see [54]). The usage of such type of parametrizations will make it possible to carry out the present analysis of the data accumulated within the range of intermediate x values, which is presently under active considerations.

Support by the National Natural Science Foundation of China (Grant No. 11575254) is acknowledged. A.V.K. and B.G.S. thank Institute of Modern Physics for invitation. A.V.K. is also grateful to the CAS President’s International Fellowship Initiative (Grant No. 2017VMA0040) for support. The work of A.V.K. and B.G.S. was in part supported by the RFBR Foundation through the Grant No. 16-02-00790-a.

References

- [1] M. Arneodo, Phys. Rept. **240**, 301 (1994); P. R. Norton, Rept. Prog. Phys. **66**, 1253 (2003).
- [2] K. Rith, Subnucl. Ser. **51**, 431 (2015); S. Malace, D. Gaskell, D. W. Higinbotham and I. Cloet, Int. J. Mod. Phys. E **23**, no. 08, 1430013 (2014); K. Kovarik *et al.*, Phys. Rev. D **93**, no. 8, 085037 (2016).
- [3] J. J. Aubert *et al.*, European Muon Collab., Phys. Lett. **123B**, 275 (1983).
- [4] K. J. Eskola, H. Paukkunen and C. A. Salgado, JHEP **0904**, 065 (2009); M. Hirai, S. Kumano and T.-H. Nagai, Phys. Rev. C **76**, 065207 (2007); D. de Florian, R. Sassot, P. Zurita and M. Stratmann, Phys. Rev. D **85**, 074028 (2012); K. Kovarik *et al.*, Phys. Rev. D **93**, no. 8, 085037 (2016).

- [5] K. J. Eskola, P. Paakkinen, H. Paukkunen and C. A. Salgado, *Eur. Phys. J. C* **77**, no. 3, 163 (2017).
- [6] H. Khanpour and S. Atashbar Tehrani, *Phys. Rev. D* **93**, no. 1, 014026 (2016).
- [7] S. Dulat *et al.*, *Phys. Rev. D* **93**, no. 3, 033006 (2016); L. A. Harland-Lang *et al.*, *Eur. Phys. J. C* **75**, no. 5, 204 (2015); R. D. Ball *et al.*, NNPDF Collab., *JHEP* **1504**, 040 (2015); A. Accardi *et al.*, *Eur. Phys. J. C* **76**, no. 8, 471 (2016); *Phys. Rev. D* **93**, no. 11, 114017 (2016); P. Jimenez-Delgado and E. Reya, *Phys. Rev. D* **89**, no. 7, 074049 (2014); S. Alekhin *et al.*, arXiv:1701.05838 [hep-ph].
- [8] V. N. Gribov and L. N. Lipatov, *Sov. J. Nucl. Phys.* **15**, 438 (1972); *Sov. J. Nucl. Phys.* **15**, 675 (1972); L. N. Lipatov, *Sov. J. Nucl. Phys.* **20**, 94 (1975); G. Altarelli and G. Parisi, *Nucl. Phys. B* **126**, 298 (1977); Y. L. Dokshitzer, *Sov. Phys. JETP* **46**, 641 (1977).
- [9] A. V. Kotikov, V. G. Krivokhizhin and B. G. Shaikhatdenov, arXiv:1612.06412 [hep-ph].
- [10] V. G. Krivokhizhin and A. V. Kotikov, *Phys. Atom. Nucl.* **68**, 1873 (2005); *Phys. Part. Nucl.* **40**, 1059 (2009).
- [11] S. A. Kulagin and R. Petti, *Nucl. Phys. A* **765**, 126 (2006); *Phys. Rev. C* **90**, no. 4, 045204 (2014).
- [12] R. Wang, X. Chen and Q. Fu, *Nucl. Phys. B* **920**, 1 (2017); R. Wang and X. Chen, *Phys. Lett. B* **743**, 267 (2015); X. Chen, J. Ruan, R. Wang, P. Zhang and W. Zhu, *Int. J. Mod. Phys. E* **23**, no. 10, 1450058 (2014); W. Zhu, R. Wang and J. Ruan, *Int. J. Mod. Phys. E* **26**, 1750009 (2017).
- [13] R. L. Jaffe, F. E. Close, R. G. Roberts and G. G. Ross, *Phys. Lett.* **134B**, 449 (1984); O. Nachtmann and H. J. Pirner, *Z. Phys. C* **21**, 277 (1984).
- [14] F. E. Close, R. L. Jaffe, R. G. Roberts and G. G. Ross, *Phys. Rev. D* **31** (1985) 1004.
- [15] F. E. Close, R. G. Roberts and G. G. Ross, *Phys. Lett.* **129B**, 346 (1983); R. L. Jaffe, *Phys. Rev. Lett.* **50**, 228 (1983).
- [16] S. A. Kulagin, EPJ Web Conf. **138**, 01006 (2017).
- [17] L. Mankiewicz, A. Saalfeld, and T. Weigl, *Phys. Lett. B* **393**, 175 (1997).
- [18] A.V. Kotikov and G. Parente, *Nucl. Phys. B* **549**, 242 (1999).
- [19] A. De Rújula, S. L. Glashow, H. D. Politzer, S.B. Treiman, F. Wilczek, A. Zee, *Phys. Rev. D* **10**, 1649 (1974); R.D. Ball and S. Forte, *Phys. Lett. B* **336**, 77 (1994).
- [20] C. Adloff *et al.*, H1 Collab., *Nucl. Phys. B* **497**, 3 (1997); *Eur. Phys. J. C* **21**, 33 (2001); S. Chekanov *et al.*, ZEUS Collab., *Eur. Phys. J. C* **21**, 443 (2001).
- [21] A.M. Cooper-Sarkar *et al.*, *Int. J. Mod. Phys. A* **13**, 3385 (1998); A.V. Kotikov, *Phys. Part. Nucl.* **38**, 1 (2007) [Erratum-ibid. **38**, 828 (2007)].
- [22] F. D. Aaron *et al.*, H1 and ZEUS Collab., *JHEP* **1001** (2010) 109.
- [23] A. V. Kotikov and B. G. Shaikhatdenov, *Phys. Part. Nucl.* **44**, 543 (2013); *Phys. Atom. Nucl.* **78**, no. 4, 525 (2015); *Phys. Part. Nucl.* **48**, no. 5, 829 (2017).
- [24] A.Yu. Illarionov, A. V. Kotikov, and G. Parente, *Phys. Part. Nucl.* **39**, 307 (2008).
- [25] G. Cvetic, A.Yu. Illarionov, B.A. Kniehl, and A.V. Kotikov, *Phys. Lett.* **B679**, 350 (2009).
- [26] A. M. Cooper-Sarkar *et al.*, PoS DIS **2016** (2016) 013; I. Abt *et al.*, *Phys. Rev. D* **94**, no. 3, 034032 (2016); Z. Zhang, H1 and ZEUS Collab., *Acta Phys. Polon. Supp.* **8**, 957 (2015).
- [27] B. Badelek, J. Kwiecinski and A. Stasto, *Z. Phys. C* **74**, 297 (1997); Y. A. Simonov, *Phys. Atom. Nucl.* **74**, 1223 (2011).
- [28] D. V. Shirkov and I. L. Solovtsov, *Phys. Rev. Lett.* **79**, 1209 (1997).

- [29] D. V. Shirkov, Phys. Part. Nucl. Lett. **10**, 186 (2013).
- [30] A. Deur, S. J. Brodsky and G. F. de Teramond, Prog. Part. Nucl. Phys. **90**, 1 (2016).
- [31] A.V. Kotikov, A. V. Lipatov, and N. P. Zotov, J. Exp. Theor. Phys. **101**, 811 (2005);
A. V. Kotikov, V. G. Krivokhizhin and B. G. Shaikhatdenov, Phys. Atom. Nucl. **75** (2012) 507.
- [32] A. V. Efremov, Phys. Lett. B **174**, 219 (1986).
- [33] A. V. Kotikov, Sov. J. Nucl. Phys. **50**, 127 (1989).
- [34] P. Bolzoni, B. A. Kniehl and A. V. Kotikov, Phys. Rev. Lett. **109**, 242002 (2012); Nucl. Phys. B **875**, 18 (2013); B. A. Kniehl and A. V. Kotikov, arXiv:1702.03193 [hep-ph].
- [35] S. Alekhin, S.A. Kulagin and R. Petti, Phys. Rev. D **96**, no.5, 054005 (2017).
- [36] M. Arneodo *et al.*, New Muon Collab., Nucl. Phys. B **441**, 12 (1995); Nucl. Phys. B **481**, 3 (1996); P. Amaudruz *et al.*, New Muon Collab., Nucl. Phys. B **441**, 3 (1995).
- [37] M. R. Adams *et al.*, E665 Collab., Z. Phys. C **67**, 403 (1995); K. Ackerstaff *et al.*, HERMES Collab., Phys. Lett. B **475**, 386 (2000) Erratum: [Phys. Lett. B **567**, 339 (2003)].
- [38] L. Frankfurt, V. Guzey and M. Strikman, Phys. Rev. C **95**, no. 5, 055208 (2017).
- [39] N. Armesto, J. Phys. G **32**, R367 (2006); H. Paukkunen, arXiv:1704.04036 [hep-ph].
- [40] M. Winn, arXiv:1704.04217 [nucl-ex].
- [41] F. D. Aaron *et al.* [H1 Collaboration], Phys. Lett. B **686**, 91 (2010); Eur. Phys. J. C **65**, 89 (2010).
- [42] S. Chekanov *et al.* [ZEUS Collaboration], Eur. Phys. J. C **65**, 65 (2010); H. Abramowicz *et al.* [ZEUS Collaboration], JHEP **1409**, 127 (2014).
- [43] C. Adolph *et al.* [COMPASS Collaboration], Phys. Rev. D **87**, no. 5, 052018 (2013); Eur. Phys. J. C **72**, 2253 (2012).
- [44] H. Abramowicz *et al.* [H1 and ZEUS Collaborations], Eur. Phys. J. C **73**, no. 2, 2311 (2013).
- [45] J. J. Aubert *et al.* [European Muon Collaboration], Nucl. Phys. B **213**, 31 (1983); Phys. Lett. **110B**, 73 (1982); Phys. Lett. **94B**, 96 (1980).
- [46] S. Frixione, M. L. Mangano, P. Nason and G. Ridolfi, Phys. Lett. B **348**, 633 (1995); S. Frixione, P. Nason and G. Ridolfi, Nucl. Phys. B **454**, 3 (1995)
- [47] E. Chudakov *et al.*, J. Phys. Conf. Ser. **770**, no. 1, 012042 (2016); PoS DIS **2016**, 143 (2016).
- [48] A. Y. Illarionov, B. A. Kniehl and A. V. Kotikov, Phys. Lett. B **663**, 66 (2008); A. Y. Illarionov and A. V. Kotikov, Phys. Atom. Nucl. **75**, 1234 (2012).
- [49] V. N. Baier, V. S. Fadin and V. A. Khoze, Sov. Phys. JETP **23**, 104 (1966); V. G. Zima, Yad. Fiz. **16**, 1051 (1972); V. M. Budnev, I. F. Ginzburg, G. V. Meledin and V. G. Serbo, Phys. Rept. **15**, 181 (1975).
- [50] E. Witten, Nucl. Phys. B **104**, 445 (1976); J. P. Leveille and T. J. Weiler, Nucl. Phys. B **147**, 147 (1979); M. A. Shifman, A. I. Vainshtein and V. I. Zakharov, Nucl. Phys. B **136**, 157 (1978).
- [51] A. V. Kotikov, A. V. Lipatov, G. Parente and N. P. Zotov, Eur. Phys. J. C **26**, 51 (2002).
- [52] M. Gluck, E. Reya and M. Stratmann, Nucl. Phys. B **422** (1994) 37.
- [53] C. Patrignani *et al.* [Particle Data Group], Chin. Phys. C **40**, no. 10, 100001 (2016).
- [54] A. Y. Illarionov, A. V. Kotikov, S. S. Parzycki and D. V. Peshekhonov, Phys. Rev. D **83**, 034014 (2011).